First Evidence for Different Freeze-Out Conditions for Kaons and Antikaons Observed in Heavy-Ion Collisions

A. Förster,[2] F. Uhlig,[2] I. Böttcher,[4] M. Dębowski,[5,6] F. Dohrmann,[6] E. Grosse,[6,7] P. Koczoń,[1] B. Kohlmeyer,[4] F. Laue,[1,*]
M. Menzel,[4] L. Naumann,[6] H. Oeschler,[2] W. Scheinast,[6] E. Schwab,[1] P. Senger,[1] Y. Shin,[3] H. Ströbele,[3] C. Sturm,[2,1]
G. Surówka,[1,5] A. Wagner,[6] and W. Waluś[5]

(KaoS Collaboration)

[1]Gesellschaft für Schwerionenforschung, D-64220 Darmstadt, Germany
[2]Technische Universität, Darmstadt, D-64289 Darmstadt, Germany
[3]Johann Wolfgang Goethe-Universität, D-60325 Frankfurt am Main, Germany
[4]Phillips Universität, D-35037 Marburg, Germany
[5]Jagiellonian University, PL-30059 Kraków, Poland
[6]Forschungszentrum Rossendorf, D-01314 Dresden, Germany
[7]Technische Universität, Dresden D-0l062 Dresden, Germany

Differential production cross sections of K^- and K^+ mesons have been measured in Ni + Ni and Au + Au collisions at a beam energy of 1.5 A GeV. The K^-/K^+ ratio is found to be nearly constant as a function of the collision centrality and system size. The spectral slopes and the polar emission pattern differ for K^- and K^+ mesons. These observations indicate that K^+ mesons decouple earlier from the fireball than K^- mesons.

        PACS numbers: 25.75.Dw

Heavy-ion collisions provide the unique possibility to study baryonic matter well above saturation density. The conditions inside the dense reaction zone and the in-medium properties of hadrons can be explored by measuring the particles created in such collisions [1,2]. In particular, strange mesons produced at beam energies below or close to the NN threshold are well suited for these studies. The yield of K^+ mesons as measured in Au + Au collisions at the heavy-ion synchrotron (SIS) at GSI in Darmstadt [3] constrains the nuclear matter equation of state [4]. The pronounced patterns of the elliptic and directed flow of kaons provide evidence for the existence of a repulsive kaon-nucleon in-medium potential [5,6]. The K^-/K^+ ratio is enhanced in heavy-ion collisions as compared to proton-proton collisions [7,8]. In order to reproduce the measured yields, transport model calculations have to take into account density-dependent K-meson nucleon (KN) potentials corresponding to an in-medium modification of the K meson mass [9,10]. On the other hand, the measured ratios of strange particles can be explained within statistical models without any in-medium modification of the masses. These models reproduce the measured ratios by choosing an appropriate pair of values for the temperature and the baryon chemical potential assuming thereby a simultaneous chemical freeze-out [11].

Quantitative information on the production mechanisms and the properties of strange mesons in dense baryonic matter can be extracted from the phase-space distributions of K^+ and K^- mesons observed in heavy-ion collisions. In central Au + Au collisions at beam energies above 4 A GeV the spectral slopes were found to be similar for K^+ and K^- mesons [12]. The rapidity density distributions of strange mesons from central Au + Au collisions at 10.7 A GeV and Pb + Pb collisions at 158 A GeV were found to be wider for K^+ than for K^- mesons [13,14]. In both cases, the K^-/K^+ ratio is constant as a function of the collision centrality. At beam energies below the NN thresholds for strangeness production ($NN \rightarrow K^+ \Lambda N$ at $E = 1.6$ GeV, $NN \rightarrow K^+ K^- NN$ at $E = 2.5$ GeV), where in-medium effects are expected to influence the kaon production significantly, a systematic comparison of K^+ and K^- phase-space distributions has not yet been published.

In this Letter we present results of experiments on K^+ and K^- production in Ni + Ni and Au + Au collisions studied at a beam energy of 1.5 A GeV. This is the lowest beam energy where antikaons have been observed thus far in collisions between heavy nuclei. We have measured the spectral and angular distributions of strange mesons as a function of the collision centrality and have found significant differences between kaons and antikaons.

The experiments were performed with the Kaon Spectrometer (KaoS) at the heavy-ion synchrotron at GSI [15]. Because of the energy loss in the Au target (thickness 0.5 mm) the average energy of the Au beam is 1.48 A GeV. The energy loss of the Ni ions in the Ni target is negligible. In order to reach an energy of 1.5 A GeV for Au beams, an exceptional operation of the GSI accelerator facility was required: acceleration of the $^{197}Au^{63+}$ ions with the synchrotron up to an energy of 0.3 A GeV, then extraction and full stripping, then injection into the

Experimental Storage Ring (ESR) where the beam was cooled by electron cooling, then reinjection into the synchrotron and acceleration up to 1.5 A GeV.

In order to study the centrality dependence we grouped the data measured close to midrapidity ($\theta_{lab} = 40°$) into five centrality bins for both Ni + Ni and Au + Au collisions. The centrality of the collision is derived from the multiplicity of charged particles measured in the interval $12° < \theta_{lab} < 48°$. The most central collisions correspond to 5% of the total reaction cross section σ_R; the subsequent centrality bins correspond to 15%, 15%, and 25% of σ_R. The most peripheral collisions correspond to 40% of σ_R. The total reaction cross section has been derived from a measurement with a minimum bias trigger and was found to be $\sigma_R = 6.0 \pm 0.5$ b for Au + Au and $\sigma_R = 2.9 \pm 0.3$ b for Ni + Ni collisions. The corresponding number of participating nucleons, A_{part}, has been calculated from the measured reaction cross-section fractions using a geometrical model assuming a sharp nuclear surface.

Figure 1 shows the production cross sections for K^+ and K^- mesons measured close to midrapidity as a function of the kinetic energy in the center-of-momentum system for the five centrality bins in Au + Au collisions. The uppermost spectra correspond to the most central reactions. The error bars represent the statistical uncertainties of the kaon and the background events. An overall systematic

error of 10% due to efficiency corrections and beam normalization has to be added. The solid lines represent the function $Ed^3\sigma/dp^3 = CE\exp(-E/T)$ fitted to the data. C is a normalization constant and the exponential describes the energy distribution with T as the inverse slope parameter.

The spectra presented in Fig. 1 exhibit a distinct difference between K^- and K^+: The slopes of the K^- spectra are steeper than those of the K^+ spectra. The inverse slope parameters T are displayed in the upper panel of Fig. 2 as a function of the number of participating nucleons A_{part}. T increases with increasing centrality and is found to be significantly lower for antikaons than for kaons, even for the most central collisions. When interpreting spectral slopes one should keep in mind that they are influenced by both the random and the collective motion of the particles (temperature and flow). The radial-flow contribution to the slope depends on the particle mass and hence cannot cause a difference between the K^+ and the K^- spectra. The temperature contribution to the slope is determined at kinetic freeze-out, i.e., at the time when the particles cease to interact.

The kaon multiplicity is defined for each centrality bin as $M = \sigma_K/\sigma_r$ with σ_K the kaon production cross section and σ_r the reaction cross section of the particular event class. Figure 2 presents M/A_{part} for K^+ (second panel) and for K^- (third panel) as a function of A_{part}. For both K^+ and K^- mesons the multiplicities exhibit a similar rise with A_{part}. Moreover, M/A_{part} is found to be almost identical in Ni + Ni and Au + Au collisions. The K^-/K^+ ratio is about 0.02 below $A_{part} = 100$ and decreases slightly to about 0.015 for the most central collisions (Fig. 2, bottom panel).

Another observable sensitive to the production mechanism is the polar angle emission pattern. The deviation from isotropy of the K^+ and the K^- emission can be studied by the ratio $\sigma_{inv}(E_{CM}, \theta_{CM})/\sigma_{inv}(E_{CM}, 90°)$ as a function of $\cos(\theta_{CM})$. Here, $\sigma_{inv}(E_{CM}, \theta_{CM})$ is the invariant kaon production cross section measured at the polar angle θ_{CM} in the center-of-momentum frame and $\sigma_{inv}(E_{CM}, 90°)$ is the one measured at $\theta_{CM} = 90°$. Because of limited statistics we considered only Au + Au collisions grouped into two centrality bins: near-central (impact parameter $b < 6$ fm) and noncentral collisions ($b > 6$ fm). Figure 3 displays the anisotropy ratio for K^+ (top panel) and K^- (bottom panel) and for near-central (right-hand side) and noncentral collisions (left-hand side). For an isotropic distribution this ratio would be constant and identical to 1.

The solid lines in Fig. 3 represent the function $1 + a_2\cos^2(\theta_{CM})$ which is fitted to the experimental distributions with the values of a_2 given in the figure. In near-central collisions the K^- mesons exhibit an isotropic emission pattern, whereas the emission of K^+ mesons is forward-backward peaked. The angular distributions observed for K^+ and K^- in Ni + Ni collisions at 1.93 A GeV are similar to the ones presented in Fig. 3
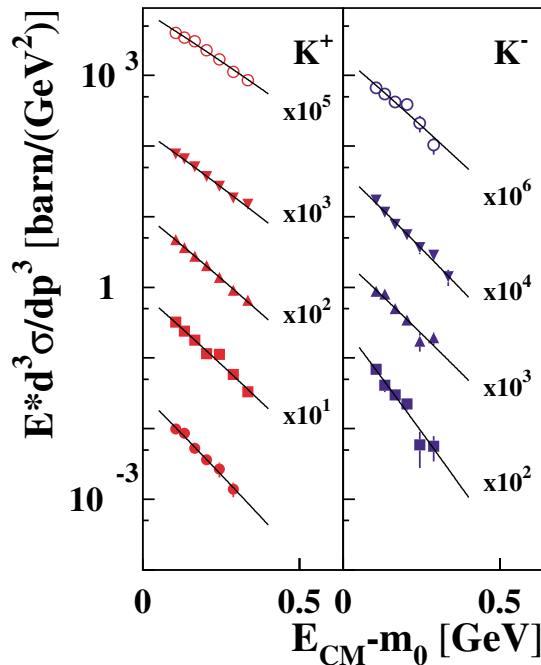

FIG. 1 (color online). Differential production cross sections for K^+ (left) and for K^- mesons (right) from Au + Au collisions at 1.5 A GeV for different centrality bins as a function of the kinetic energy in the c.m. system. The data were measured at a laboratory angle of $\theta_{lab} = 40°$ which covers midrapidity. The spectra correspond to bins of decreasing centrality (from top to bottom; see text)
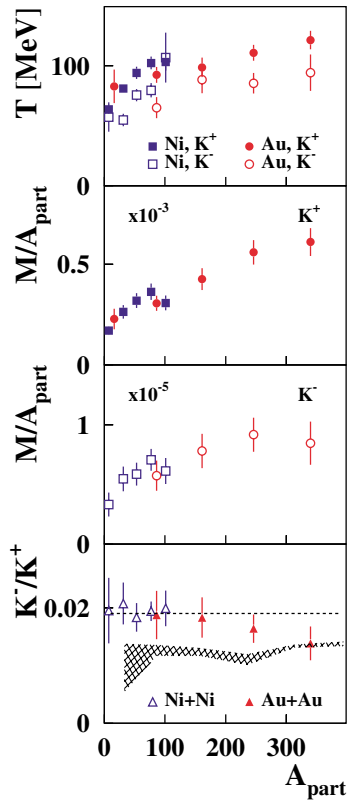
FIG. 2 (color online). Top panel: Inverse spectral slope parameters of K^+ (solid symbols) and of K^- mesons (open symbols) produced in Ni + Ni (squares) and Au + Au collisions (circles) at 1.5 A GeV as a function of the number of participating nucleons. Second and third panels: Multiplicity per number of participating nucleons $A_{\rm part}$ of K^+ and of K^- as a function of $A_{\rm part}$ both for Ni + Ni (squares) and for Au + Au (circles) at a beam energy of 1.5 A GeV. The data were taken at a laboratory angle of $\theta_{\rm lab} = 40°$. Bottom panel: The ratio of the K^- to K^+ multiplicities as a function of $A_{\rm part}$. The dashed line represents the result of a statistical model calculation [11]. The crosshatched area corresponds to the results of a QMD transport model calculation for in-medium masses of K mesons [16].

[17]. The measured emission patterns indicate that the antikaons — in contrast to the kaons — have lost the memory of the beam direction for central heavy-ion collisions.

In the following we compare our data to the results of theoretical calculations. Statistical models using a canonical formulation of strangeness conservation predict a constant K^-/K^+ ratio as a function of system size for heavy-ion collisions at SIS beam energies [11]. The result of such a calculation is shown in the bottom panel of Fig. 2 as a dashed line [11]. In this case a baryochemical potential of $\mu = 770$ MeV and a chemical freeze-out temperature of $T = 63$ MeV was assumed. Measured inverse slope parameters refer to thermal freeze-out and are substantially larger: $T(K^+) = 103 \pm 6$ MeV and $T(K^-) = 93 \pm 6$ MeV for near-central Ni + Ni collisions, and $T(K^+) = 116 \pm 7$ MeV and $T(K^-) = 90 \pm 8$ MeV for
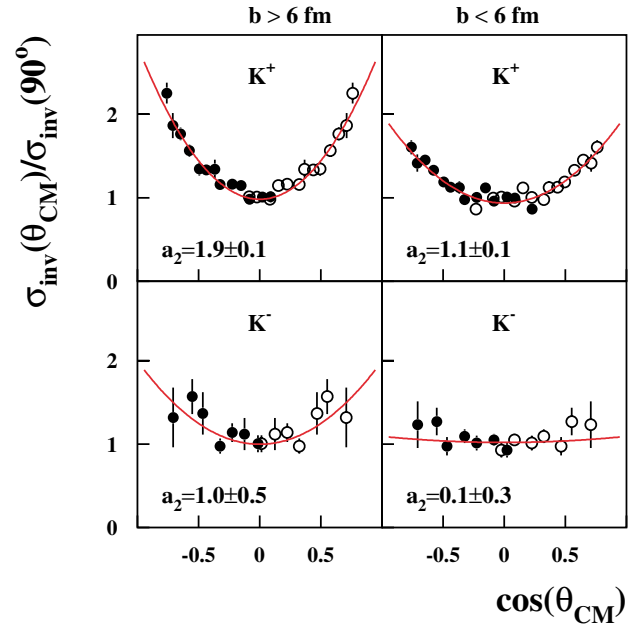
FIG. 3 (color online). Polar angle distributions of K^+ (upper panel) and of K^- mesons (lower panel) produced in peripheral (left) and near-central (right) Au + Au collisions at 1.5 A GeV. The data were taken at laboratory angles between $\theta_{\rm lab} = 32°$ and 72°. Full data points are measured and mirrored at $\cos(\theta_{CM}) = 0$ (open circles). The lines correspond to the function $1 + a_2\cos^2(\theta_{CM})$ fitted to the data (see text). The resulting values for a_2 are indicated.

near-central Au + Au collisions (corresponding to the average value of the two most central bins in Fig. 2, top panel).

The observation of different spectral slopes or mean energy for K^+ and K^- mesons is at variance with a scenario in which both kaons and antikaons have the same flow velocity and thermal energy at chemical freeze-out. In consequence, the statistical model does not offer a consistent explanation for both the yields and spectral slopes of K^+ and K^- mesons. The difference in spectral slopes rather indicates that K^+ and K^- mesons decouple from the fireball sequentially due to their very different KN inelastic cross sections.

Microscopic transport models predict that the kaons and the hyperons are produced via processes like $NN \rightarrow K^+YN$ or $\pi N \rightarrow K^+Y$ with $Y = \Lambda, \Sigma$ in the early phase of a heavy-ion collision [4,9,18]. The K^+ mesons leave the reaction volume with little rescattering because of their long mean free path. Therefore, the K^+ mesons probe the early, dense, and hot phase of the collision and have been used to obtain information on the nuclear equation of state [3,4]. Within the transport calculations the production of antikaons proceeds predominantly via strangeness-exchange reactions $\pi Y \rightarrow K^- N$ [9,16,19]. The mean free path of the K^- mesons is about 1.5 fm in nuclear matter due to absorption via reactions like $K^- N \rightarrow Y\pi$. However, via the inverse reaction ($\pi Y \rightarrow K^- N$) the antikaons may reappear again thus propagating
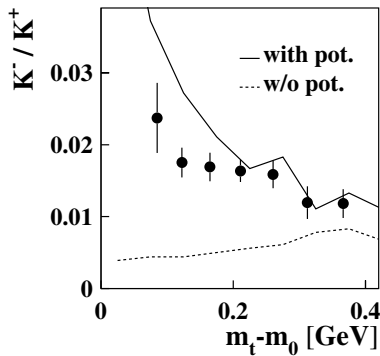
FIG. 4. K^- to K^+ ratio as a function of the transverse mass for near-central ($b < 5$ fm) Au + Au collisions at 1.5 A GeV around midrapidity. The curves represent the predictions of a transport model calculation (BUU) including in-medium potentials (solid line) and for free K meson masses (dashed line). The data (solid circles) were taken at $\theta_{lab} = 40°$

to the surface of the fireball. Consequently, the yields of K^+ and K^- mesons are both related to the hyperon yield, but the observed K^- mesons in average are produced later than the K^+ mesons [16].

The various transport calculations do not yet provide a consistent picture concerning the in-medium properties of antikaons. Recent quantum molecular dynamics (QMD) model calculations predict a rather weak sensitivity of the K^- yield on the K^-N potential [16]. The calculations result in a K^-/K^+ ratio which systematically underestimates the experimental data (see the crosshatched area in the bottom panel of Fig. 2) [16]. This result is based on the assumption of in-medium K^+ and K^- masses. A very similar result is obtained for free masses. On the other hand, Boltzmann-Uehling-Uhlenbeck (BUU) calculations need to take into account an attractive in-medium K^-N potential in order to explain the K^- yields [9,10]. Predictions of a BUU model calculation [10] for the K^-/K^+ ratio as a function of transverse mass for near-central Au + Au collisions at 1.5 A GeV are shown in Fig. 4 together with our experimental results. A similar result was found for Ni + Ni collisions at 1.93 A GeV [20]. As demonstrated in Fig. 4, the calculations assuming free K meson masses (dashed line) and in-medium masses (solid line) clearly disagree. In this case the differences in spectral slope are caused by the opposite mean-field potentials of kaons and antikaons (see also [21]). However, both the QMD [16] and the BUU models [10,21] use a rather simple parametrization of the effective mass of K^+ and K^- mesons in nuclear matter. New theoretical concepts are required to improve the interpretation of experimental data. This is expected from the next generation of transport calculations which take into account off-shell effects like in-medium spectral functions and in-medium cross sections [22,23].

In summary, we have presented differential cross sections and phase-space distributions of kaons and anti-

kaons produced in heavy-ion collisions at 1.5 A GeV. We observed the following features: (i) The K^-/K^+ yield ratio is quite independent of A_{part} both for Ni + Ni and Au + Au collisions, (ii) in near-central collisions K^- mesons are emitted almost isotropically whereas K^+ mesons exhibit a forward-backward enhanced emission pattern, and (iii) the inverse slope parameters are significantly smaller for K^- than for K^+ mesons even for the most central Au + Au collisions. These findings indicate that (i) the production mechanisms of K^+ and K^- mesons are correlated by strangeness-exchange reactions, (ii) K^- mesons undergo many collisions before leaving the fireball and, as a consequence, (iii) K^- and K^+ mesons experience different freeze-out conditions.

*Present address: Brookhaven National Laboratory, USA.
[1] J. Aichelin and C. M. Ko, Phys. Rev. Lett. **55**, 2661 (1985).
[2] G. Q. Li, C. H. Lee, and G. E. Brown, Phys. Rev. Lett. **79**, 5214 (1997).
[3] C. Sturm et al., Phys. Rev. Lett. **86**, 39 (2001).
[4] C. Fuchs et al., Phys. Rev. Lett. **86**, 1974 (2001).
[5] Y. Shin et al., Phys. Rev. Lett. **81**, 1576 (1998).
[6] P. Crochet et al., Phys. Lett. B **486**, 6 (2000).
[7] R. Barth et al., Phys. Rev. Lett. **78**, 4007 (1997).
[8] F. Laue et al., Phys. Rev. Lett. **82**, 1640 (1999).
[9] W. Cassing and E. L. Bratkovskaya, Phys. Rep. **308**, 65 (1999).
[10] G. Q. Li and G. E. Brown, Phys. Rev. C **58**, 1698 (1998).
[11] J. Cleymans, H. Oeschler, and K. Redlich, Phys. Rev. C **59**, 1663 (1999); Phys. Lett. B **485**, 27 (2000).
[12] L. Ahle et al., Phys. Rev. C **58**, 3523 (1998).
[13] N. Herrmann et al., Annu. Rev. Nucl. Part. Sci. **49**, 581 (1999).
[14] J. Bächler et al., Nucl. Phys. **A661**, 45c (1999).
[15] P. Senger et al., Nucl. Instrum. Methods Phys. Res., Sect. A **327**, 393 (1993).
[16] C. Hartnack, H. Oeschler, and J. Aichelin, Phys. Rev. Lett. **90**, 102302 (2003); (private communication).
[17] M. Menzel et al., Phys. Lett. B **495**, 26 (2000).
[18] J. Aichelin, Phys. Rep. **202**, 233 (1991).
[19] C. M. Ko, Phys. Lett. **138B**, 361 (1984).
[20] K. Wisniewski et al., Eur. Phys. J. A **9**, 515 (2000).
[21] E. L. Bratkovskaya, W. Cassing, and U. Mosel, Phys. Lett. B **424**, 244 (1998).
[22] M. Lutz, Phys. Lett. B **426**, 12 (1998).
[23] W. Cassing et al., nucl-th/0304006.